Antiviral Research 93 (2012) 175–184

Contents lists available at SciVerse ScienceDirect

Antiviral Research

journal homepage: www.elsevier.com/locate/antiviral

Inhibition or deficiency of cathepsin B leads defects in HIV-1 Gag pseudoparticle release in macrophages and HEK293T cells ☆

Soon-Duck Ha, Sangwook Park, Clayton James Hattlmann, Stephen Dominic Barr, Sung Ouk Kim *

Department of Microbiology and Immunology and Centre for Human Immunology, Siebens-Drake Research Institute, University of Western Ontario, London, Ontario, Canada N6G 2V4

ARTICLE INFO

Article history:
Received 2 June 2011
Revised 11 October 2011
Accepted 17 November 2011
Available online 26 November 2011

Keywords:
HIV
Cathepsin B
Trafficking
Egress
Enveloped virus

ABSTRACT

Human immunodeficiency virus type 1 (HIV-1) egresses from infected cells through utilizing the host membrane budding mechanisms. Assembly of HIV-1 Gag particles occurs on membranes where the Gag multimers subsequently bud off and form enveloped viral particles. In certain cell types such as macrophages, HIV-1 Gag particles have shown to be released into intracellular virus containing compartments (VCC) such as late endosomes, multivesicular bodies (MVBs) or invaginated plasma membrane pockets. Here, we showed that macrophages or HEK293T cells treated with the cathepsin B (CTSB)-specific inhibitor CA-074Me or cells deficient in CTSB failed to release HIV-1 Gag pseudoparticles into the extracellular environment. Based on immunofluorescence and electron microscopy, these cells retained the pseudoparticles in heterogeneous intracellular VCC. CA-074Me was also able to inhibit propagation of two enveloped viruses, herpes simplex virus and influenza A virus, but not non-enveloped enterovirus. These results suggest that CTSB is required for the efficient release of HIV-1 Gag pseudoparticles and targeting CTSB can be a new therapeutic strategy for inhibiting egress of HIV-1 and other enveloped viruses.

1. Introduction

Assembly and egress of HIV-1 are multistep processes highly regulated by viral and cellular factors. The major structural protein of HIV-1 is the polyprotein Gag (Pr55Gag) which is cleaved into multi-subunits (matrix, capsid, spacer peptide 1, nucleocapsid, spacer peptide 2, and p6) by HIV-1 protease during the budding process. However, exogenous expression of Pr55Gag without other viral components is sufficient for the formation of non-infectious virus-like Gag particles (Garoff et al., 1998). Newly synthesized HIV-1 Gags are trafficked to the site of budding where the endosomal sorting complex required for transport (ESCRT) complexes are recruited (Chu et al., 2009; Morita and Sundquist, 2004). The ESCRT complexes, comprised ESCRT-0, -1, -2, and -3, and several ESCRT-accessory factors, execute the sorting and inward budding of mono-ubiquitinated molecules/cargoes into intralumenal vesicles, forming the tetraspanins (such as CD63)-enriched multivesicular bodies (MVBs) (Williams and Urbe, 2007). HIV-1 Gag utilizes the ESCRT complexes to egress from the plasma membrane (Baumgartel et al., 2011; Jouvenet et al., 2011) or to bud into intracellular virus containing compartments (VCC) (Benaroch et al., 2010; Chu et al., 2009). It is well established that, in T lymphocytes and some epithelial cells (Hermida-Matsumoto and Resh, 2000; Jouvenet et al., 2006; Ono and Freed, 2004; Palmer et al., 1985), HIV-1 Gag buds from the plasma membrane, likely through glycolipid and cholesterol enriched lipid rafts (Waheed and Freed, 2009). However, in other cell types such as macrophages and certain fibroblasts, HIV-1 Gag was shown to bud into intracellular VCC at least in part positive for MVBs or late endosome markers, such as tetraspanins, lysosomal-associated membrane protein-I and MHC-II, before being released from cells (Kramer et al., 2005; Ono and Freed, 2004; Orenstein, 2002; Pelchen-Matthews et al., 2003; Raposo et al., 2002; Resh, 2005; Tang et al., 2009). However, in macrophages, recent studies also suggested that the intracellular vesicles are in fact extensions of the plasma membrane connected through thin micro-channel conduits (Bennett et al., 2009; Deneka et al., 2007; Jouvenet et al., 2006; Welsch et al., 2011, 2007). To date, the presence of the conduits in other cell types, characteristics of the unique intracellular plasma membrane pockets and the contribution of the pockets in viral release are still being investigated (Benaroch et al., 2010).

HIV-1 also intercepts the autophagy process for its virion assembly and egress (Dinkins et al., 2010; Kyei et al., 2009). Autophagy is a cell survival and host defense mechanism during starvation and microbial invasion, respectively, by clearing damaged organelles, macromolecular aggregates and intracellular microbes by forming double-membrane vacuoles, termed autophagosomes (He and Klionsky, 2009). Autophagosomes typi-

☆ This work was supported by Canadian Institute of Health Research (CIHR) Operating Grant (MOP93551) to S.O.K., and Grants from the Ontario HIV Treatment Network (OHTN)/CIHR (HIV/AIDS HBF107546) to S.D.B.

* Corresponding author. Tel.: +1 519 850 2961; fax: +1 519 661 2046.
E-mail address: sung.kim@schulich.uwo.ca (S.O. Kim).

0166-3542/$ - see front matter © 2011 Elsevier B.V. All rights reserved.
doi:10.1016/j.antiviral.2011.11.009

cally mature into amphisomes or autolysosomes after fusing with MVBs (Fader and Colombo, 2009) or lysosomes (Noda et al., 2009), respectively. Extensive studies have identified more than 20 autophagy ('Atg') gene products involved in the process. Central to the process is the conjugation of phosphatidylethanolamine lipid to the microtubule-associated protein 1 light chain 3 (LC3; a mammalian homolog of yeast Atg8). The lipidated LC3s associate with autophagosomal membranes, and promote autophagosome generation and maturation (Nakatogawa et al., 2007). The mechanisms underlying the incorporation of HIV-1 Gag particles into the autophagosomes and the release of HIV-1 Gag particles into the extracellular environment are still largely unknown.

Cathepsin B (CTSB) is a lysosomal cysteine protease primarily involved in the degradation of lysosomal proteins (McGrath, 1999). Several studies including ours have shown that CTSB is also involved in various cellular functions including myoblast differentiation (Jane et al., 2002), arachidonic acid release (Foghsgaard et al., 2002), cell death (McGrath, 1999), inflammasome activation (Jin and Flavell, 2010), the delivery of tumor necrosis factor-α containing cargo to the plasma membrane (Ha et al., 2008) and the release of anthrax toxins into the cytoplasm (Ha et al., 2010). Thus, we examined the effects of the CTSB-specific inhibitor CA-074Me on HIV-1 Gag pseudoparticle release, and found that certain cells including macrophages and HEK293T cells treated with CA-074Me or macrophages deficient in CTSB failed to release HIV-1 Gag pseudoparticles into the extracellular environment.

2. Experimental procedures

2.1. Materials and Reagents

The synthetic cathepsin B inhibitor CA-074Me ([(2S,3S)-3-propylcarbamoyloxirane-2-carbonyl]-L-isoleucyl-L-proline methyl ester, $C_{19}H_{31}N_3O_6$) and cholera toxin B subunit-FITC conjugate (C-1655) were purchased from Peptide Institute Inc. (Osaka, Japan) and Sigma–Aldrich (St. Louis, MO), respectively. The plasmids for GFP-LC3 (an N-terminal GFP-conjugated LC3) and pPr55Gag-CFP (a C-terminal cyan fluorescent protein fused to HIV-1 Gag) were obtained from Drs. Yoshimori (National Institute for Basic Biology, Okazaki, Japan) and Spearman (Vanderbilt University School of Medicine, Nashville). The following reagents were provided through the NIH AIDS Research and Reference Reagent Program (Division of AIDS, NIAID, NIH): the plasmid encoding codon-optimized Gag (p96ZM651gag-opt) from Drs. Li, Gao and Hahn (Gao et al., 2003); pPr55Gag-GFP containing EGFP fused to the C-terminal of rev-independent Gag from Dr. Resh (catalog #11468) (Schwartz et al., 1992); antiserum to HIV-1 p17 from Dr. Spearman (catalog# 4811); the HIV-1 p24 monoclonal antibody (183-H12-5C) from Dr. Chesebro and Wehrly (Chesebro et al., 1992; Toohey et al., 1995; Wehrly and Chesebro, 1997). pR9 was obtained from Dr. R. Bushman (University of Pennsylvania). All plasmid transfections were performed using Lipofectamine 2000 (Invitrogen). Antibodies for p38 were obtained from Cell Signaling Technologies (Pickering, ON), beta-actin antibodies from Rockland Inc. (Gilbertsville, PA) and human CD63 antibody from BD Biosciences.

2.2. Cell culture

HEK293T cells were grown in DMEM containing 10% heat-inactivated fetal bovine serum (Sigma), 10 mM MEM non-essential amino acids solution, 100 U/mL penicillin G sodium, 100 μg/mL streptomycin sulfate and 1 mM sodium pyruvate (DMEM complete medium). Cells were grown at 37 °C in the humidified atmosphere of 5% CO_2. GHOST(3)X4/R5 reporter cells were obtained from Drs. M.N. KewalRamani and D.R. Littman (Division of AIDS, NIAID, NIH) through the NIH AIDS Research and Reference Reagent Program. Primary bone marrow-derived macrophages (BMDM) (Weischenfeldt and Porse, 2008) and bone marrow-derived immortalized macrophages (BMDIM) (Ha et al., 2008) from wild-type C57 BL/6 mice or cathepsin B-deficient mice were prepared as previously described. These cells were grown in complete RPMI 1640 medium containing 10% heated-inactivated fetal bovine serum (Sigma), 10 mM MEM non-essential amino acids solution, 100 U/mL penicillin G sodium, 100 μg/mL streptomycin sulfate and 1 mM sodium pyruvate at 37 °C in the humidified atmosphere of 5% CO_2.

2.3. Quantitation of Gag particle release

The plasmid pGag-GFP (1.2 μg for 0.8×10^6 HEK293T cells or 4.0 μg for 2.5×10^6 BMDIM) was transfected into the cells by Lipofectamine 2000 (Invitrogen). Cell culture medium was changed at 8 h post-transfection and cells were then incubated with fresh culture medium containing either DMSO or CA074-Me for another 18 h, unless mentioned otherwise. Total cell lysates and Gag pseudoparticles released into the cell culture medium were prepared as previously described (Barr et al., 2008) to quantify Gag pseudoparticles. Briefly, Gag pseudoparticles released into the medium were pelleted by centrifugation (20,000*g*) for 90 min at 4 °C over a 500 μl cushion of 20% sucrose. The pellets were lysed with ice-cold lysis buffer (50 mM Tris–HCl (pH 7.4), 150 mM NaCl, I mM EDTA, 1% Triton X-100, 0.1% SDS) and subsequently used for Western blotting.

2.4. Total cell lysate preparation and Western blotting Analysis

Total cell lysate preparation and immunoblotting procedures were performed as previously described (Barr et al., 2008; Ha et al., 2008). Briefly, cells were lysed with the ice-cold lysis buffer containing Complete Protease Inhibitor Cocktail (Complete Mini EDTA-free, Roche) for 10 min. Cell lysates were then centrifuged at 12,500 rpm for 15 min at 4 °C. The supernatants were separated by SDS–polyacrylamide gels, followed by transfer onto nitrocellulose membranes (BIO-RAD). The membranes were blocked with 5% (w/v) skim milk for 1 h at room temperature and then incubated overnight at room temperature with primary antibodies. The membranes were washed with TBS buffer (50 mM Tris–HCl, 150 mM NaCl, pH 7.5) containing 0.08% Tween20, incubated with secondary antibody for 1 h (Pierce Biotech, Rockford, IL) and developed using an enhanced chemiluminescence detection system (ECL; Pierce).

2.5. Immunofluorescence staining and Intracellular Gag-particle trafficking analysis

Plasmids (1.2 μg for 0.7×10^6 HEK293T cells; 3.5 μg for 2.0×10^6 BMDIM) encoding HIV-1 Gag-GFP, Gag-CFP, GFP-LC3 or replication-competent HIV-1 provirus (pR9; 2 μg/2.0×10^6 cells) were transfected into HEK293T cells and BMDIM from wild-type (*Ctsb*$^{+/+}$) or cathepsin B-deficient (*Ctsb*$^{-/-}$) mice by Lipofectamine 2000 (Invitrogen). At 8 h post-transfection, cells were changed with fresh media and grown at 37 °C for 14–18 h with DMSO or CA-074Me, unless mentioned otherwise. Cells were fixed for 20 min in PBS containing 4% formaldehyde and washed twice with PBS. Cells were then observed through Bio-Rad Radiance 2000 two-photon fluorescence confocal microscopy or ZEISS 510 META confocal microscopy. Images were obtained using LaserSharp 2000 software (Hertfordshire, UK) or ZEN software. For immunofluorescence staining, fixed cells were treated with 10% blocking reagent for 60 min at room temperature and immunolabelled with

antibodies against p24CA or human CD63. Endogenous CD63 was detected by immunofluorescence using biotinylated anti-mouse IgG and Texas-red streptavidin (Vector Laboratories Inc.). For plasma membrane staining, cells were incubated with FITC-conjugated cholera toxin B subunit (CB-FITC; 1 μg/ml in PBS) for 15 min on ice and fixed with 4% formaldehyde. Co-localization of Gag-GFP, Gag-CSF, CB-FITC and CD63 were visualized by Bio-Rad Radiance 2000 two-photon fluorescence confocal microscopy, and images were obtained and analyzed using Lasersharp 2000 software. For co-localization analysis, spatially-calibrated images were analyzed using the "Co-localization Threshold" plugin of the ImageJ 1.43u 64-bit version software (NIH, Bethesda, MD) and automatic thresholding and statistical significance testing for spatial intensity correlation analysis (Costes et al., 2004). The Pearson's correlation coefficient of co-localized volumes measures the correlation between the intensities of the two labels in the co-localized voxels and is used to express the extent of co-localization where a value of 1.0 represents perfect correlation.

2.6. Infectious HIV-1 Virion Measurements

HEK293T cells were transfected with replication-competent proviral plasmid (pR9) using Lipofectamine 2000 (Invitrogen). Culture medium was removed 10 h post-transfection and replaced with fresh propagation medium containing CA-074Me or DMSO. Approximately 14 h later the medium was replaced with fresh medium without CA-074Me or DMSO and cultured for an additional 24 h, after which supernatants were harvested and clarified by centrifugation (800*g* for 15 min at 4 °C). Virus-containing supernatants were used to infect GHOST(3)X4/R5 reporter cells in the presence of 10 μg/ml hexadimethrine bromide (Polybrene; Sigma, H9268). Twenty-four hours post-infection, culture medium was replaced with fresh medium for an additional 24 h. Cells were harvested in PBS containing 10 mM EDTA, fixed in 2% formaldehyde for 10 min, and analyzed by flow cytometry for GFP expression using a BD FACSCalibur and BD CellQuest Pro software.

2.7. Infections and Immunfluorescence stainings for herpes simplex virus (HSV), Influenza A virus, Enterovirus

Clinical isolates of HSV1/2 (uncharacterized), influenza A virus and enterovirus (provided by R. Wheeler, Department of Virology, St. Joseph's Hospital, London, Canada) were adsorbed for 1 h on H&V Mix (MRC-5 and CV1 cells), R-Mix (A549 and Mv1Lu cells) and E-Mix (A549 and sBGMK cells) hybrid cells (Diagnostic Hybrids, Athens, Ohio), respectively. Cells were then further incubated for 18–24 h with fresh medium with DMSO or CA-074Me. After washing with PBS, cells were fixed with methanol at room temperature for 10 min and infected cells were analyzed using direct fluorescent-antibody (DFA) test kits (CHEMICON international), following the manufacturer's instructions. Primary antibodies for immunostaining influenza A (pan-specific, uncharacterized) and HSV (155 kD major capsid protein) were from Light DIAGNOSTICS™ #5307 and #5095, repectively (CHEMICON international). For enterovirus, the primary antibodies (pan-specific, uncharacterized) were from Light DIAGNOSTICS™ #3360 and the secondary antibodies conjugated FITC anti-mouse IgG were Light DIAGNOSTICS™ catalog #5008. Cells were observed under the fluorescence Axioscope 2 (Zeiss) microscope with green filter and 40× objective, and images were acquired using the Eclipse software (Nikon). Green fluorescence cells were counted as virus-infected cells.

2.8. Electron Microscopy

HEK293 cells and BMDIMs from wild type ($Ctsb^{+/+}$) or cathepsin B-deficient ($Ctsb^{-/-}$) mice were transfected with pGag-GFP (9.0 μg for 8.0×10^6 HEK293T cells; 16.0 μg for 1.0×10^7 BMDIM), washed with PBS twice, and fixed with 2.5% glutaraldehyde in 0.1 M sodium cacodylate buffer for 2 h at room temperature. Grids with specimen were prepared by the transmission electron microscope facility at the University of Western Ontario (Canada), and micrographs were taken with a transmission electron microscope. Briefly, after fixing with 2.5% glutaraldehyde, Cells were washed with 0.1 M cacodylate buffer three times, and cells were further fixed with 1% osmium tetroxide in 0.1 M cacodylate buffer for 1 h, and then rinsed with 0.1 M cacodylate buffer. Cells were enrobed in 5% Noble Agar and washed with distilled water five times, further fixing with 2% uranyl acetate for 2 h, followed by dehydration in 50% (15 min), 70% (16 h), 85% (15 min), 95% (15 min), and two changes of 100% ethanol each 15 min. They were then cleared by two changes of propylene oxide each 15 min and infiltrated with epon resin:propylene oxide (1:1) for 3 h, epon resin:propylene oxide (3:1) for 16 h, and two changes with pure epon resin for total 6 h. Thin sections were mounted on grids, and examined under the electron microscope (Philips CM-10 80 Kv and AMT Digital Camera).

3. Results

3.1. The cathepsin B (CTSB) inhibitor CA-074Me prevents the extracellular release of HIV-1 Gag by retaining the viral particle in CD63-positive compartments

We first examined the role of CTSB in HIV-1 Gag particle release using CA-074Me in HEK293T cells. Cells were transfected with a GFP-tagged HIV-1 Gag (Pr55Gag-GFP) expression vector and the release of Gag pseudoparticles was analyzed in the presence or absence of CA-074Me. As shown in Fig 1A (upper panel), the release of Pr55Gag-GFP into the cell culture medium was diminished by CA-074Me in a dose-dependent manner. In contrast, the intracellular levels were increased by CA-074Me treatments (Fig. 1A, lower

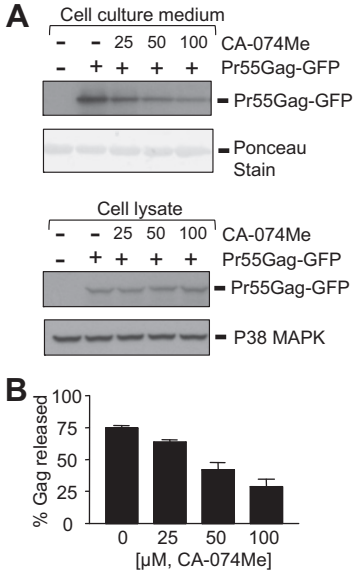

Fig. 1. The CTSB inhibitor CA-074Me inhibits Gag release in HEK293T cells. HEK293T cells were transfected with pPr55Gag-GFP as described in 'Section 2' and incubated with DMSO or varying concentrations of CA-074Me as indicated in the figure. (A) Cell lysates and cell culture supernatants were prepared and immunoblotted against anti-p24CA antibodies. For loading controls, a non-specific Ponceau staining (cell culture media) or immunobloting for p38 MAPK (cell lysates) were used. (B) Densitometric analysis of each immunoblot against Gag-p24CA was performed using NIH-image program. Relative densities of p24-immunoreactivities were normalized to loading controls and% of Gag pseudoparticle release to total production was calculated. Data show the mean ± S.D. (n=3).

panel). Based on densitometry analysis of the bands, the overall Gag pseudoparticle release was diminished by CA-074Me up to 25% of total GAG production in a dose-dependent manner (Fig. 1B). CA-074Me had no apparent cytotoxic effects on HEK293T cells in these experimental conditions (Supplemental Fig. 1S, A). Since HIV-1 Gag was shown to traffic to CD63-positive vesicles (Joshi et al., 2009; Perlman and Resh, 2006), we examined whether Pr55Gag-GFP accumulated in CD63-positive vesicles in CA-074Me-treated cells. As shown in Fig. 2A, Pr55Gag-GFP-positive puncta were mostly localized closed to the plasma membrane and partially co-localized with the CD63-positive puncta up to about 22% (upper panels); however, in the presence of CA-074Me (25 μM), Pr55Gag-GFP-positive puncta were greatly increased in number and size, about 55% of which were co-localized with CD63 (lower panels). We also examined whether Pr55Gag accumulated in autophagosomes in the presence of CA-074Me. For this study we used the CFP-fused Pr55Gag vector construct (Pr55Gag-CFP) in lieu of Pr55Gag-GFP in order to co-transfect together with the GFP-fused LC3 construct (GFP-LC3). After 26 h transfection with Pr55Gag-CFP and GFP-LC3 expression vectors, GFP-LC3 was mainly localized in the nucleus, as expected (Drake et al., 2010), and Pr55Gag-CFP was mainly detected in the plasma membrane (Fig. 2B, upper panels). However, in the presence of CA-074Me, GFP-LC3 was detected in punctated forms which were co-localized

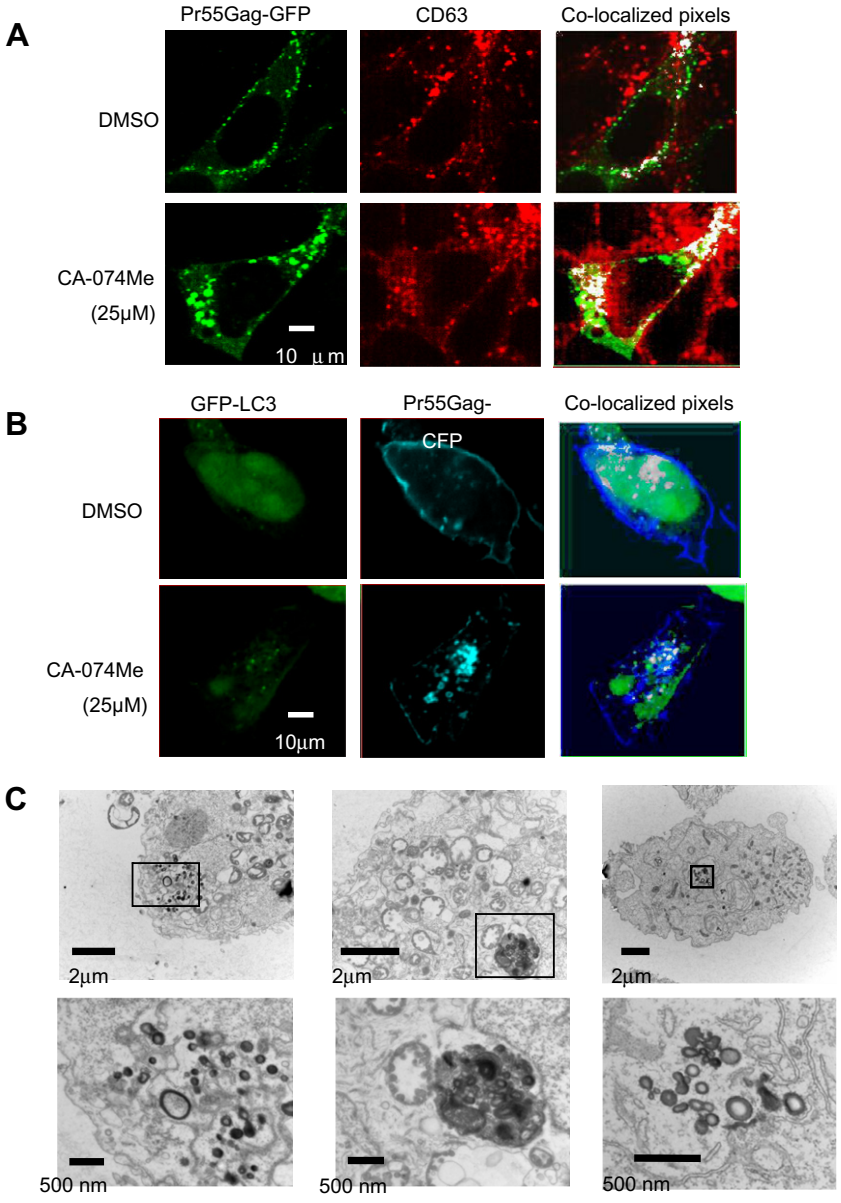

Fig. 2. CA-074Me treatment causes an accumulation of Gag particles in virus containing compartments including CD63-positive vesicles. (A) HEK293T cells were transfected with pPr55Gag-GFP as described in 'Section 2' and incubated with DMSO or 25 μM of CA-074Me. Cells were then fixed and immunostained with anti-CD63 antibody. Localization of Gag-GFP and CD63 were visualized and analyzed using the Bio-Rad Radiance 2000 confocal microscope, LaserSharp 2000 software. Using the images, co-localization of Gag-GFP with CD63-positive puncta was analyzed using the "Co-localization Threshold" analysis of the Image J 1.43u 16-bit version software as described in 'Section 2'. *R* values (the pearson's correlation coefficient) of all the analyzes are between 0.68 and 0.70. Images are representative results of more than three independent experiments. (B) Cathepsin B deficiency causes the enhanced co-localization of Gag-CFP and GFP-LC3-II. HEK293T cells were co-transfected with pGFP-LC3 and pPr55Gag-CFP, and changed with fresh media at 8 h post-transfection. Cells were incubated at 37 °C for another 18 h in the presence of DMSO (upper panel) or CA-074Me (25 μM; lower panel) and fixed with 4% formaldehyde. Images were acquired and analyzed using confocal microscope (ZEISS 510 META) and ZEN software. (C) HEK293T cells were transfected with pPr55Gag-GFP and changed with fresh media 8 h after the transfections. Cells were then incubated with or without CA-074Me for 18 h, and ultrastructures of the cells were visualized using transmission EM as described in 'Section 2'.

with Pr55Gag-CFP-positive puncta (Fig. 2B, lower panels). The ultrastructure of HIV-1 Gag particle containing vesicles was further resolved using electron microscopy (Fig. 2C). Non-treated cells showed several extracellular Gag pseudoparticles and few intracellular Gag-containing vesicles (Supplement Fig. 2S); whereas, cells treated with CA-074Me showed a large number of Gag-like particles accumulated in membrane ruffled areas (Fig. 2C, left column), large vacuoles (middle column) or double membrane vacuoles (right column). A previous study suggested that the intracellular accumulation of HIV-1 Gag was mainly due to uptake of released HIV-1 Gag pseudoparticles at later times and the intracellular accumulation was completely blocked by the actin polymerization inhibitor cytochalasin D (Jouvenet et al., 2006). We also examined the effect of cytochalasin D in the release of Pr55Gag in CA-074Me treated cells. Consistent with their report, cytochalasin D had no effects on the release of Pr55Gag (Supplemental Fig. 3S) and Pr55Gag was mostly localized at the plasma membrane (data not shown). However, CA-074Me treatments inhibited the release of the Pr55Gag pseudoparticles regardless the presence or absence of cytochalasin D, suggesting that the decrease of Pr55Gag in the cell culture medium and the increase in intracellular compartments were not likely due to reuptake of the pseudoparticles. Collectively, these Western blots, and confocal and electron microscopy data suggest that cells treated with CA-074Me accumulated Gag pseudoparticles in intracellular compartments, before being released into the extracellular environment.

3.2. The CTSB inhibitor CA-074Me prevents HIV-1 egress by retaining the viral particle in intracellular compartments partially positive for CD63

To further examine the effect of CA-074Me on HIV-1 particle release, HEK293T cells were transfected with a plasmid encoding replication-competent HIV-1 provirus (pR9) and, 10 h post-transfection, cells were further cultured with or without CA-074Me (20 μM) for 14 h. Immunostaining against HIV-1 and CD63 using antibodies against p24 capsid (CA) and human CD63, respectively, showed that, although overall intensities for CD63 were similar between non-treated and CA-074Me-treated cells, the intensities for HIV-1 were much higher in CA-074Me-treated cells than those of non-treated (Fig. 3A, left panel). At a higher magnification view, HIV-1 Gag was found to be localized predominantly at the plasma membrane and modestly in intracellular vesicles in non-treated cells; whereas, in cells treated with CA-074Me, HIV-1 Gags were mainly found in intracellular compartments in part positive for CD63 (Fig. 3A, right panel). To quantify viral release, the replication-competent HIV-1 viral particles were collected from each cell culture medium and then used to infect GHOST(3)X4/R5 reporter cells. Consistent with the image data, the amounts of HIV-1 released by cells exposed to 10 and 25 μM concentrations of CA-074Me were about 50% and 25%, respectively, of those of non-treated cells (Fig. 3B). Although we cannot rule out the effect of CA-074Me on viral infectivity, these data suggest that replication-competent HIV-1 also failed to egress in the presence of CA-074Me.

3.3. CTSB-deficient mouse macrophages or CA-074Me-treated THP-1 cells failed to cleave and release Pr55Gags

Since CA-074Me could have off-target effects, wild-type ($CTSB^{+/+}$) and CTSB-deficient ($CTSB^{-/-}$) bone marrow-derived immortalized macrophages (BMDIM) were transfected with Pr55Gag-GFP plasmids and the release of Pr55Gag pseudoparticles was analyzed (Fig. 4A). Similar to HEK293T cells, BMDIM deficient in CTSB ($CTSB^{-/-}$) failed to release Pr55Gag-GFP to cell culture media (Fig. 4A, upper and lower left panel). To our surprise, both of the released and intracellular Pr55Gag-GFP were cleaved in $CTSB^{+/+}$ but not in $CTSB^{-/-}$ BMDIM which retained full length Pr55Gag-GFP (Pr55Gag-GFP, indicated in Fig. 4A upper right panel) in cell lysates. Similar results were also obtained in CTSB-deficient bone marrow-derived primary macrophages (Fig. 4D). Western blot analysis using HIV-1 matrix protein p17 antibody also showed similar results as shown with anti-GFP antibody (Fig. 4A, middle panel), indicating that both N-terminus and C-terminus portions of cleaved pr55Gag-GFP were released into cell culture medium. To rule out that the cleavage and release of Pr55Gag-GFP was not a mouse cell-specific event, the human monocytic cell line THP-1 cells were treated with varying doses of CA-074Me, and Pr55Gag-GFP cleavage and release were examined. Unlike mouse BMDIM and BMDM, transfection efficiency was much lower in THP-1 cells and multiple non-specific bands cross-reacting with anti-GFP antibodies were visible in cell lysates due to high amount of protein loading in the gel; however, distinct cleaved Pr55Gag-GFP and full length Pr55Gag-GFP bands were visible (Fig. 4B, indicated by arrows) in cell lysates. In THP-1 cells, only cleaved Gag-GFP was found in the cell culture medium and CA-074Me inhibited the release of Gag-GFP in a dose-dependent manner (Fig. 4B, lower panel). In correlation with the Gag-GFP release, increasing

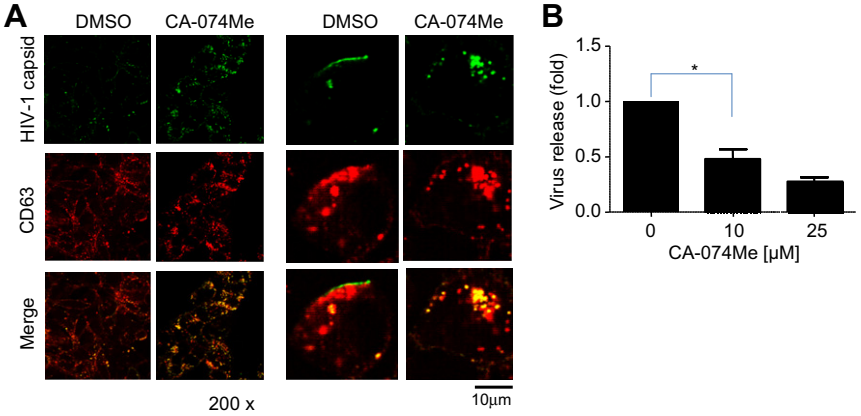

Fig. 3. CA-074Me retained HIV-1 virus in CD63-positive MVB-like compartments and inhibits the viral egress in HEK293T cells. (A) Analysis of HIV-1 Gag localization in the presence or absence of CA-074Me. HEK293T cells were transfected with pR9 as described in 'Section 2'. After 10 h transfection, cell culture medium was replaced with fresh medium containing DMSO or CA-074Me (25 μM) for 14 h. Cells were then further cultured for an additional 24 h in fresh medium and fixed with 4% formaldehyde. Gag localization was assessed by confocal immunofluorescence using anti-p24 and anti-CD63. (B) Effect of CA-074Me treatment on infectious HIV-1 virion release. HEK293T cells were transfected with pR9 and then treated with DMSO or CA-074Me. Drug-containing medium was replaced with fresh medium and virus was allowed to accumulate in the supernatant for 24 h. Virus released into the supernatant was quantified using GHOST(3)X4/R5 reporter cells. GFP-expressing cells were measured by flow cytometry. Data are expressed as the mean ± S.D. ($n = 3$ data are expressed as the mean ± S.D; $^*p < 0.05$; Student's t-test).

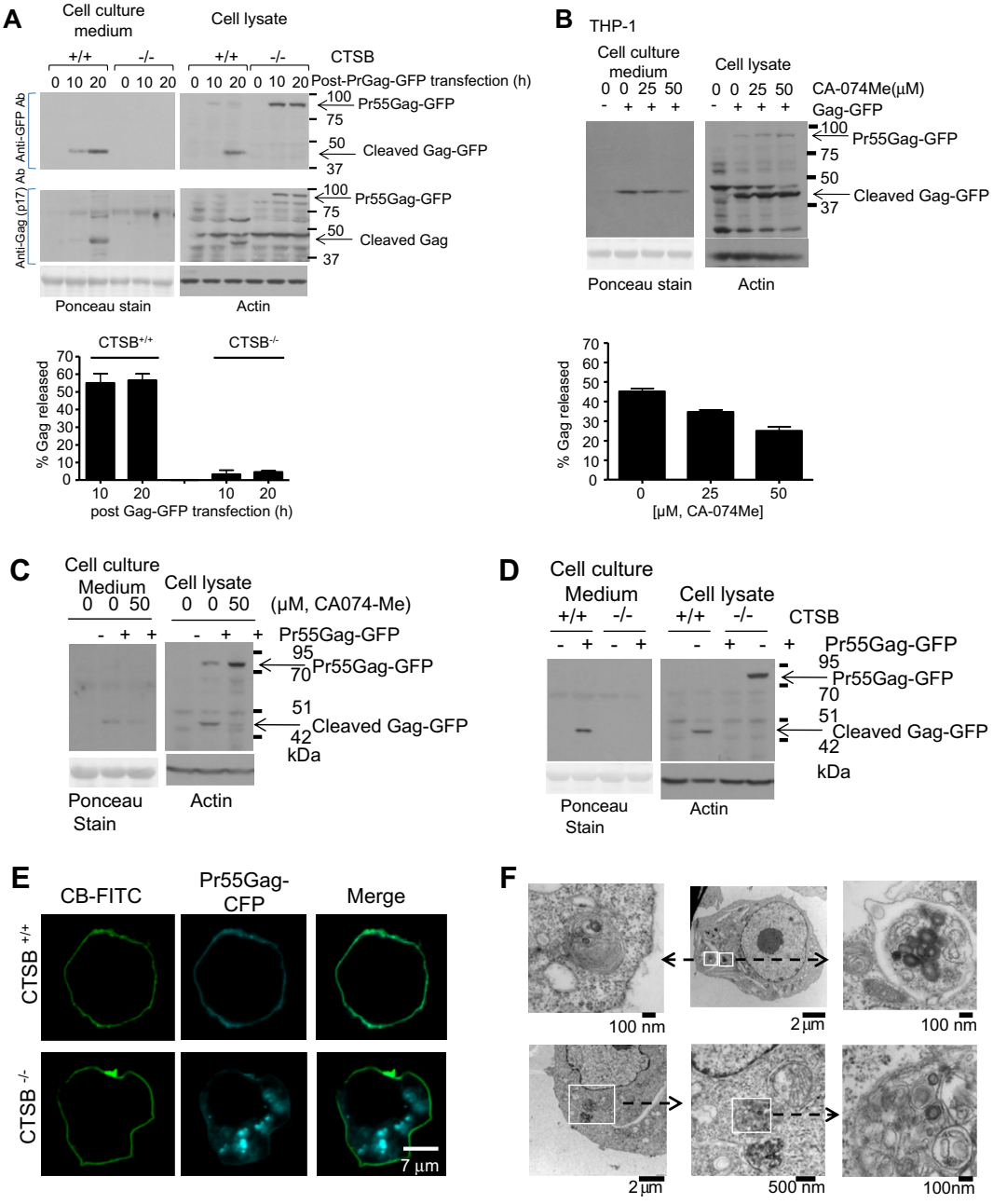

Fig. 4. Ctsb$^{-/-}$ macrophages accumulate Pr55Gag pseudoparticles in intracellular compartments and are defective in releasing Pr55Gag pseudoparticles. (A) BMDIM from wild-type (*Ctsb*$^{+/+}$) or cathepsin B-deficient (*Ctsb*$^{-/-}$) mice were transfected with pPrGag-GFP for 8 h and incubated with fresh media for the time indicated in the figure. (B) Human monocytic leukemia cell line THP-1 cells were transfected with pPr55Gag-GFP for 8 h and incubated with fresh media with or without CA-074Me for 18 h. (A and B) Cell lysates and Gag-GFP pseudoparticles in cell culture medium were immunoblotted using anti-GFP antibody. For loading controls, ponceau staining (cell culture media) and beta-actin immunoblotting (cell lysates) were used. Densitometric analysis of each immunoblot against Gag-p24CA was performed using NIH-image program. Relative densities of p24-immunoreactivities were normalized to loading controls and% of Gag pseudoparticle release to total production was calculated. Data show the mean ± S.D. (n = 3). (C) Bone marrow-derived primary mouse macrophages were transfected with the pPr55Gag-GFP plasmid for 8 h. Cell were then cultured with or without CA074-Me (50 μM) for the next 26 h. (D) Bone marrow-derived primary macrophages from wild-type (CTSB$^{+/+}$) or cathepsin B-deficient (CTSB$^{-/-}$) mice were transfected with the pPr55Gap-GFP plasmid for 40 h. (A–D) Cell lysates and cell culture supernatants were prepared and immunoblotted against anti-GFP or anti-Gag p17 antibodies as indicated in the figure. For loading controls, a non-specific ponceau staining (cell culture media) or immunobloting against actin was used. Only cleaved Gag-GFP was detected in cell culture media of non-treated wild-type macrophages; whereas, full length Gap-GFP was detected in lysates prepared from macrophages treated with CA074-Me or deficient in CTSB. (E) BMDIM from wild-type (*Ctsb*$^{+/+}$) or cathepsin B-deficient (*Ctsb*$^{-/-}$) mice were transfected with pGag-CFP for 8 h and incubated with fresh media for 14 h. Cells were then washed with PBS and fixed after staining with FITC conjugated cholera toxin B subunit (CB-FITC) for plasma membrane. Images were acquired and analyzed using confocal microscope (ZEISS 510 META) and ZEN software. (F) BMDIM from cathepsin B-deficient (*Ctsb*$^{-/-}$) mice were transfected with pGag-GFP for 8 h and incubated with fresh media for 18 h. Cells were then fixed with 2.5% glutaraldehyde and visualized using transmission EM as described in 'Section 2'.

amounts of full length Gag-GFP were detected in cell lysates prepared from cells treated with increasing concentrations of CA-074Me. CA-074Me also inhibited the release of Gag-GFP in primary bone marrow-derived macrophages (Fig. 4C) but not in Jurkat T cells (Supplemental Fig. 4S). No apparent cytotoxic effects of CA-074Me at concentrations examined were detected in BMDM and THP-1 cells (Supplemental Fig. 1S, B & C).

We further examined the location of Pr55Gag in macrophages using fluorescence microscopy and EM (Fig. 4E and F, respectively). Similar to HEK293T cells, Pr55Gag-CFP was mainly localized in the

plasma membrane in CTSB$^{+/+}$ BMDIM; whereas, CTSB$^{-/-}$ cells accumulated Pr55Gag-CFP in intracellular compartments which was distinct from the plasma membrane (Fig. 4E, lower panels). EM analysis also suggested that Gag-like particles were accumulated in MVBs (Fig. 4F, upper right panel and lower panels) and autophagosomes (Fig. 4F, upper left panel) in CTSB$^{-/-}$ BMDIM. Collectively, these data show that CTSB$^{-/-}$ macrophages, like CA-074Me-treated HEK293T cells, failed to release HIV-1 Gag pseudoparticles and retained the pseudoparticles in VCC.

3.4. CA-074Me inhibits the propagation of clinically isolated enveloped herpes simplex virus (HSV) and influenza A virus, but not non-enveloped enterovirus

The biogenesis of MVBs has been shown to be involved in the assembly and egress in many enveloped virus (Calistri et al., 2009, 2007; Hobman, 1993). To examine the involvement of CTSB in the egress of other viruses, herpes simplex virus (HSV), influenza A virus and enterovirus were propagated in the corresponding susceptible cell lines in the presence or absence of CA-074Me (Fig. 5). HSV is a large DNA-containing enveloped virus and MVB biogenesis was shown to be important for its envelopment and egress (Calistri et al., 2007). Influenza A virus is a segmented negatively stranded enveloped RNA virus that buds from the polarized surface of virus-infected cells (Barman et al., 2001). Enterovirus is a non-enveloped single stranded RNA virus. As shown in Fig. 5, CA-074Me substantially prevented propagation of the two enveloped viruses but not the non-enveloped enterovirus, based on the number of cells infected by virus. Immunofluorescence analysis using antibodies for the HSV p155 major capsid protein, together with Evans blue for control membrane staining, showed a punctated pattern in CA-074Me-treated infected cells (Fig. 5A); whereas non-treated control cells showed a diffused staining pattern throughout the cytoplasm. Immunofluorescene images using pan-specific influenza virus antibodies (Fig. 5B) and blended antibodies recognizing enterovirus (Fig. 5C) showed a diffused pattern in the cytoplasm without apparent differences in both non-treated and CA-074Me-treated cells (Fig. 5C). Although it is unknown whether CA-074Me prevented egress processes of HSV and influenza A virus, these results suggest that CA-074Me had inhibitory effects on the propagation of enveloped HSV and influenza A virus but not non-enveloped enterovirus.

4. Discussion

CTSB is primarily known as a lysosomal cysteine protease involved in the degradation of cellular proteins; however, several studies including ours have shown its involvement in various cellular functions (Foghsgaard et al., 2002; Jane et al., 2006; Jin and Flavell, 2010; McGrath, 1999) including trafficking of vesicles (Ha et al., 2010, 2008). This study further showed that CTSB was required for the release of HIV-1 Gag pseudoparticles and possibly other enveloped viruses including HSV and influenza A virus (Fig. 5). HIV-1 Gag particles are synthesized in the cytoplasm and bud off from the plasma membranes and/or intracellular VCC, or being enclosed into autophagosomes in certain cells including macrophages, HEK293T, fibroblasts, COS and HeLa cells (Dong et al., 2005; Nydegger et al., 2003; Ono and Freed, 2004; Sherer et al., 2003; Tang et al., 2009). As previously mentioned, unlike in T lymphocytes, HIV-1 Gags were shown to egress into invaginated plasma membrane pockets in macrophages (Bennett et al., 2009; Deneka et al., 2007; Jouvenet et al., 2006; Welsch et al., 2011, 2007). However, as recently reviewed in detail by Benaroch et al. (2010), the characteristics and contribution of the plasma membrane pockets in HIV-1 Gag egress are yet to be determined.

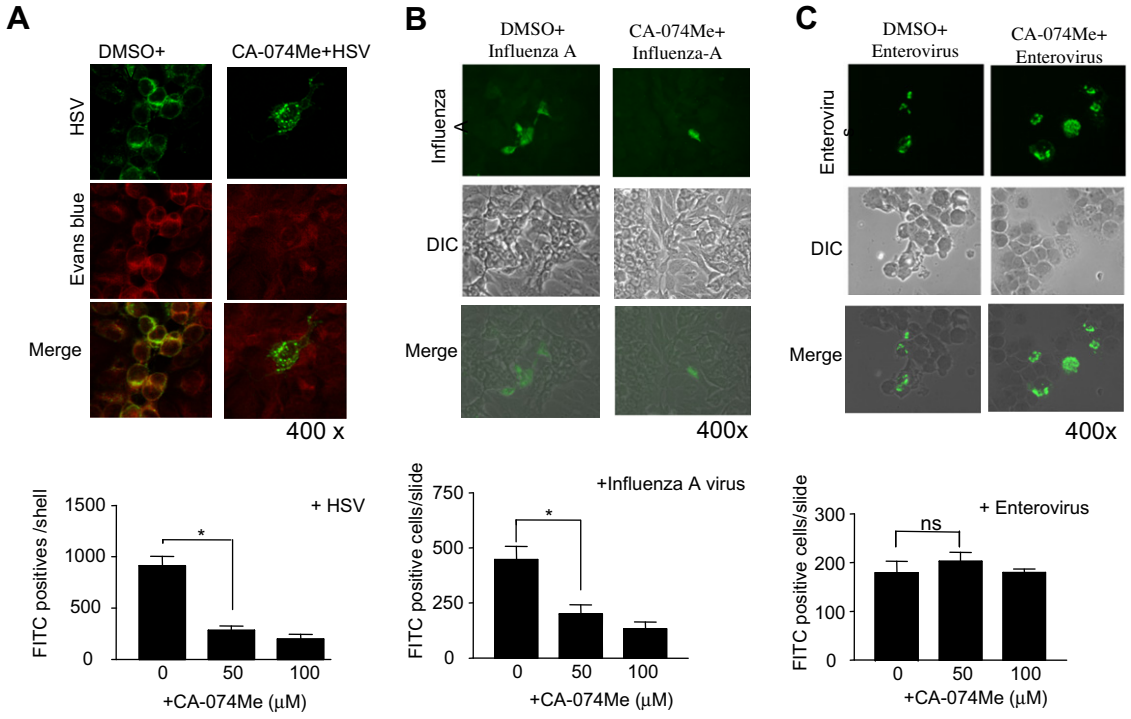

Fig. 5. The CTSB inhibitor CA-074Me prevents propagation of HSV and influenza A virus but not enterovirus. (A–C) Clinical isolates of HSV, influenza A virus and enterovirus were inoculated into H&V Mix shell vials (MRC-5-CV1), R-Mix shell vials (A549/Mv1Lu) and super E-Mix shell vials (A549-sBGMK), respectively, for 1 h at 37 °C in 5% CO_2 incubator. Cells were then treated with DMSO or CA-074Me as indicated in the Figure and fixed as described in 'Section 2'. Virus-infected cells were visualized by immunofluorescent staining using monoclonal antibodies raised against viral proteins specific for the types. Immunofluorescent staining were processed as described in 'Section 2' and the numbers of infected cells were quantified by counting the number of cells with green fluorescence using an Axioscope 2 (Zeiss) microscope and Eclipse software (Nikon) under the Green or DIC. Data are expressed as the mean ± S.D. ($n = 3$, HSV and influenza A viruses; $^*p < 0.01$; ns (not significant), $p > 0.2$; Student's t-test). Representative images of three independent experiments in the presence of DMSO or 50 μM CA-074Me are shown.

For example, about 20% of HIV-1 Gag particle containing compartments were shown to be an extension of the plasma membrane; whereas the rest, 80%, of them remained to be excluded from plasma membrane staining (Benaroch et al., 2010; Jouve et al., 2007). Also, unlike in T lymphocytes, no budding events at the plasma membrane have been observed by EM in macrophages (Benaroch et al., 2010). We also were not able to detect Pr55Gag pseudoparticles budding off at the plasma membrane of macrophages.

Involvement of endosomal trafficking in HIV-1 Gag release has been implicated in Niemann-Pick type C-1 (NPC1) gene mutant cells. NPC1 protein is well known for its role in endosomal vesicle trafficking (Davies et al., 2000; Liscum, 2000), and its defects lead to impaired intra-endosomal trafficking mediated by late endosomal cholesterol accumulation (Ko et al., 2001). In cells deficient in NPC1 protein, HIV-1 release is inhibited and results in Gag accumulation in late endosomes/lysosomemal compartments (Tang et al., 2009). Previously, we found that CTSB is required for efficient autophagy efflux process and CA-074Me causes an accumulation of MVBs and autophagosomes (Ha et al., 2010). Here we showed that CA-074Me inhibited the release of Pr55Gag (Fig. 1–4) and HSV (Fig. 5A). The retained Pr55Gag pseudoparticles were accumulated as puncta, in part colocalized with CD63 or LC3, the markers of MVB and autophagosome, respectively (Fig. 2A and B). Many enveloped viruses including HIV-1 and HSV bud into the limited membranes as platforms for the assembly of viral envelope and for viral egress (Calistri et al., 2009, 2007; Hobman, 1993). In general, fusion of MVBs and autophagy with lysosomes is a degradation process of cellular components and foreign invaders. However, several evidences support that MVBs and late endosomes transiently fuse with lysosomes to form hybrid organelles which are then transported to the plasma membrane through a secretory pathway (Bright et al., 1997; Luzio et al., 2007; Mullock et al., 1998). Interestingly, HIV-1 was shown to utilize the endogenous MVB/autophagy and secretory pathways to assemble and egress (Dong et al., 2005; Kyei et al., 2009; Nydegger et al., 2003; Pelchen-Matthews et al., 2003), while suppressing the late autophagy maturation process through expressing the HIV-1 protein Nef (Kyei et al., 2009). Therefore, HIV-1 can manipulate endosomal trafficking pathways to evade destructive pathway for maximal survival inside cells and for efficient egress. At this moment, it is not clear whether cathepsin B should be present in HIV-1 Gag-containing vacuoles/MVBs for their release. To our surprise, that Pr55Gag was also cleaved in a CTSB-dependent manner before its release into the extracellular environment in mice and human macrophages (Fig. 4). Since the cleavage was not detected in HEK293T cells (Fig. 1 and Supplemental Fig. 3S), Jurkat cells (Supplemental Fig 4S) or CTSB-deficient macrophages (Fig. 4A and C), it was a CTSB-dependent phenomenon specific to macrophages. We have also examined the release of Pr55Gag-GFP in other cell types including mouse embryonic fibroblast and the primary human fibroblasts (GM00038; CORIELL INSTITUTE, New Jersey). In these cells, release of Gag particles were also blocked by CA-0874Me but no cleavage of Gag-GFP was detected (data not shown). At this moment, it is not yet clear why and when Pr55Gag-GFP was cleaved in macrophages. We tempt to speculate that, since macrophages, unlike other cells, have high basal levels of and efficient in autophagosome formation (Ha et al., 2010, 2008), Pr55Gag-GFP could have been directly targeted by CTSB through a partial lysosomal fusion with VCCs before being released extracellularly (Luzio et al., 2007). Intracellular cleavage of Pr55Gag-GFP is also consistent with the results that cleaved Gag particles were detected in both viral particles collected from the medium and cell lysates (Fig. 4A–D), and GFP was associated with the plasma membrane rather than in the cytoplasm (Fig. 4E, upper panel). We are currently investigating whether the cleavage occurs in the presence of other HIV gene products such as Nef and what the physiological significance of the cleavage is in infectivity. Based on the size of the cleaved C-terminal portion of the fragment (~45 kDa), the GFP antibody reacted fragment is expected to contain a small part of the C-terminal Gag and full length of GFP (~35 kDa). We have also examined the cleavage of Pr55Gag-CFP fusion protein using anti-Gag (p17) antibody and found similar results as shown in Fig. 4A, lower panel. Therefore, the cleavage was not specific to Pr55Gag-GFP. We are currently investigating the exact location of the cleavage, when it occurs, and how it affects viral infectivity.

Since influenza A virus is known to egress through the plasma membrane, independent of functional MVB biogenesis (Bruce et al., 2009), the inhibitory effect of CA-074Me on influenza A virus was somewhat unexpected. A recent study showed that influenza A virus budding and filament formation requires Rab11 and Rab11-family interacting protein 3 which play key roles in endosome recycling/trafficking and budding (Bruce et al., 2010), suggesting that CTSB could be involved in the transport or assembly of viral components to recycling endosomes. The recycling endosomes, which was first identified as a key component in recycling internalized transferrin and its receptor to the cell surface, are now being recognized as a key component in secretory pathways in various cell types (van Ijzendoorn, 2006).

We previously showed that CTSB is also involved in the trafficking of TNF-α-containing vesicles to the plasma membrane (Ha et al., 2008). The newly synthesized pro-TNF-α in the endoplasmic reticulum is transported from the trans-Golgi network to the plasma membrane through a recycling endosomes-mediated secretory pathway (Stow et al., 2009), which was then rapidly cleaved by TNF-α converting enzyme and released from the plasma membrane as a soluble cytokine. In fact, the release of both TNF-α (Reefman et al., 2010) and Gag particle (Amet et al., 2008) is also prevented by small interference RNA against Rab11 which plays a key role in recycling/trafficking endosomes. Therefore, we speculate that TNF-α, Gag pseudoparticles and influenza A virus are also released through a common CTSB-dependent recycling endosome-mediated secretory pathway. However, CTSB has been shown to cleave viral glycoproteins and enhance entry or replication of several viruses including Ebola and Marburg virus (Chandran et al., 2005; Sanchez, 2007), mouse hepatitis virus (Qiu et al., 2006), Nipah virus (Diederich et al., 2008) and filovirus (Sanchez, 2007). Therefore, the inhibition of HSV and influenza A virus propagation by CTSB could have occurred in steps other than egress. Further detailed studies are needed to delineate the mechanism of CA-074Me in inhibiting the propagation of HSV and influenza A virus.

Therapeutic use of CTSB inhibitors such as CA074 has been examined for treating metastatic melanoma (Matarrese et al., 2010) and suppressing T helper cell type 2 responses in animals (Maekawa et al., 1997). Although long term toxicity and the effects on humans are to be investigated, no particular toxicity was detected in experimental animals (Katunuma, 2011). This study showed that targeting CTSB, which plays a key role in vesicle trafficking, could be a new therapeutic strategy that blocks the late stage of virion egress for HIV-1 and possibly other enveloped viral infections. While preparing this manuscript, a recent study showed that CA-074Me can promote the CD4-independent mNDK HIV-1 strain entry in HeLa and 293T cells (Yoshii et al., 2011). Therefore, the effects and overall antiviral efficacy of CA-074Me in other HIV strains and HIV infection still need to be evaluated. In any case, specific blocking of viral egress from VCC can lead viral particles to lysosomal degradation, promoting antiviral immune responses through activating various intracellular immune receptors such as retinoic acid inducible gene I and melanoma differentiation-associated gene-5 (Barral et al., 2009), and presenting antigens to

CD4+ T cells through MHC-II molecules. Furthermore, dendritic cells can uptake HIV particles into MVBs, which are later released through an intrinsic exosomal pathway to infect CD4+ T cells, known as *trans*-dissemination (Izquierdo-Useros et al., 2010). The effect of CTSB inhibitors on dendritic cell *trans*-dissemination warrants further studies.

Acknowledgements

We thank Drs. K. Khazaie and D.V. KewalRamani/D.R. Littman for kindly providing CTSB$^{-/-}$ mice and Ghost(3)X4/R5 reporter cells. We also thanks Drs. T. Yoshimori, F. Bushman, M. Resh, Y. Li/F. Gao/B.H. Hahn and B. Chesebro/K Wehrly for providing GFP-LC3, pR9, pPr55Gag-GFP, p96ZM651gag-opt and the HIV-1 p24 monoclonal antibody (183-H12-5C), respectively. We also thank Dr. S. Spearman for kindly providing pPr55-CFP construct and antiserum to HIV-1 p17. We also thank Mr. Russ Wheeler for providing clinical isolates of HSV, influenza A virus and enterovirus.

Appendix A. Supplementary data

Supplementary data associated with this article can be found, in the online version, at doi:10.1016/j.antiviral.2011.11.009.

References

Amet, T., Nonaka, M., Dewan, M.Z., Saitoh, Y., Qi, X., Ichinose, S., Yamamoto, N., Yamaoka, S., 2008. Statin-induced inhibition of HIV-1 release from latently infected U1 cells reveals a critical role for protein prenylation in HIV-1 replication. Microbes Infect. 10, 471–480.

Barman, S., Ali, A., Hui, E.K., Adhikary, L., Nayak, D.P., 2001. Transport of viral proteins to the apical membranes and interaction of matrix protein with glycoproteins in the assembly of influenza viruses. Virus Res. 77, 61–69.

Barr, S.D., Smiley, J.R., Bushman, F.D., 2008. The interferon response inhibits HIV particle production by induction of TRIM22. PLoS Pathog. 4, e1000007.

Barral, P.M., Sarkar, D., Su, Z.Z., Barber, G.N., DeSalle, R., Racaniello, V.R., Fisher, P.B., 2009. Functions of the cytoplasmic RNA sensors RIG-I and MDA-5: key regulators of innate immunity. Pharmacol. Ther. 124, 219–234.

Baumgartel, V., Ivanchenko, S., Dupont, A., Sergeev, M., Wiseman, P.W., Kräusslich, H.G., Brauchle, C., Müller, B., Lamb, D.C., 2011. Live-cell visualization of dynamics of HIV budding site interactions with an ESCRT component. Nat. Cell. Biol. 13, 469–474.

Benaroch, P., Billard, E., Gaudin, R., Schindler, M., Jouve, M., 2010. HIV-1 assembly in macrophages. Retrovirology 7, 29.

Bennett, A.E., Narayan, K., Shi, D., Hartnell, L.M., Gousset, K., He, H., Lowekamp, B.C., Yoo, T.S., Bliss, D., Freed, E.O., Subramaniam, S., 2009. Ion-abrasion scanning electron microscopy reveals surface-connected tubular conduits in HIV-infected macrophages. PLoS Pathog. 5, e1000591.

Bright, N.A., Reaves, B.J., Mullock, B.M., Luzio, J.P., 1997. Dense core lysosomes can fuse with late endosomes and are re-formed from the resultant hybrid organelles. J. Cell. Sci. 110, 2027–2040.

Bruce, E.A., Medcalf, L., Crump, C.M., Noton, S.L., Stuart, A.D., Wise, H.M., Elton, D., Bowers, K., Digard, P., 2009. Budding of filamentous and non-filamentous influenza A virus occurs via a VPS4 and VPS28-independent pathway. Virology 390, 268–278.

Bruce, E.A., Digard, P., Stuart, A.D., 2010. The Rab11 pathway is required for influenza A virus budding and filament formation. J. Virol. 84, 5848–5859.

Calistri, A., Sette, P., Salata, C., Cancellotti, E., Forghieri, C., Comin, A., Göttlinger, H., Campadelli-Fiume, G., Palù, G., Parolin, C., 2007. Intracellular trafficking and maturation of herpes simplex virus type 1 gB and virus egress require functional biogenesis of multivesicular bodies. J. Virol. 81, 11468–11478.

Calistri, A., Salata, C., Parolin, C., Palù, G., 2009. Role of multivesicular bodies and their components in the egress of enveloped RNA viruses. Rev. Med. Virol. 19, 31–45.

Chandran, K., Sullivan, N.J., Felbor, U., Whelan, S.P., Cunningham, J.M., 2005. Endosomal proteolysis of the Ebola virus glycoprotein is necessary for infection. Science 308, 1643–1645.

Chesebro, B., Wehrly, K., Nishio, J., Perryman, S., 1992. Macrophage-tropic human immunodeficiency virus isolates from different patients exhibit unusual V3 envelope sequence homogeneity in comparison with T-cell-tropic isolates: definition of critical amino acids involved in cell tropism. J. Virol. 66, 6547–6554.

Chu, H., Wang, J.J., Spearman, P., 2009. Human immunodeficiency virus type-1 gag and host vesicular trafficking pathways. Curr. Top. Microbiol. Immunol. 339, 67–84.

Costes, S.V., Daelemans, D., Cho, E.H., Dobbin, Z., Pavlakis, G., Lockett, S., 2004. Automatic and quantitative measurement of protein-protein colocalization in live cells. Biophys. J. 86, 3993–4003.

Davies, J.P., Chen, F.W., Ioannou, Y.A., 2000. Transmembrane molecular pump activity of Niemann-Pick C1 protein. Science 290, 2295–2298.

Deneka, M., Pelchen-Matthews, A., Byland, R., Ruiz-Mateos, E., Marsh, M., 2007. In macrophages, HIV-1 assembles into an intracellular plasma membrane domain containing the tetraspanins CD81, CD9, and CD53. J. Cell. Biol. 177, 329–341.

Diederich, S., Thiel, L., Maisner, A., 2008. Role of endocytosis and cathepsin-mediated activation in Nipah virus entry. Virology 375, 391–400.

Dinkins, C., Arko-Mensah, J., Deretic, V., 2010. Autophagy and HIV. Semin. Cell. Dev. Biol. 21, 712–718.

Dong, X., Li, H., Derdowski, A., Ding, L., Burnett, A., Chen, X., Peters, T.R., Dermody, T.S., Woodruff, E., Wang, J.J., Spearman, P., 2005. AP-3 directs the intracellular trafficking of HIV-1 Gag and plays a key role in particle assembly. Cell 120, 663–674.

Drake, K.R., Kang, M., Kenworthy, A.K., 2010. Nucleocytoplasmic distribution and dynamics of the autophagosome marker EGFP-LC3. PLoS One 5, e9806.

Fader, C.M., Colombo, M.I., 2009. Autophagy and multivesicular bodies: two closely related partners. Cell Death Differ. 16, 70–78.

Foghsgaard, L., Lademann, U., Wissing, D., Poulsen, B., Jaattela, M., 2002. Cathepsin B mediates tumor necrosis factor-induced arachidonic acid release in tumor cells. J. Biol. Chem. 277, 39499–39506.

Gao, F., Li, Y., Decker, J.M., Peyerl, F.W., Bibollet-Ruche, F., Rodenburg, C.M., Chen, Y., Shaw, D.R., Allen, S., Musonda, R., Shaw, G.M., Zajac, A.J., Letvin, N., Hahn, B.H., 2003. Codon usage optimization of HIV type 1 subtype C gag, pol, env, and nef genes: in vitro expression and immune responses in DNA-vaccinated mice. AIDS Res. Hum. Retroviruses 19, 817–823.

Garoff, H., Hewson, R., Opstelten, D.J., 1998. Virus maturation by budding. Microbiol. Mol. Biol. Rev. 62, 1171–1190.

Ha, S.D., Martins, A., Khazaie, K., Han, J., Chan, B.M., Kim, S.O., 2008. Cathepsin B is involved in the trafficking of TNF-alpha-containing vesicles to the plasma membrane in macrophages. J. Immunol. 181, 690–697.

Ha, S.D., Ham, B., Mogridge, J., Saftig, P., Lin, S., Kim, S.O., 2010. Cathepsin B-mediated autophagy flux facilitates the anthrax toxin receptor 2-mediated delivery of anthrax lethal factor into the cytoplasm. J. Biol. Chem. 285, 2120–2129.

He, C., Klionsky, D.J., 2009. Regulation mechanisms and signaling pathways of autophagy. Annu. Rev. Genet. 43, 67–93.

Hermida-Matsumoto, L., Resh, M.D., 2000. Localization of human immunodeficiency virus type 1 Gag and Env at the plasma membrane by confocal imaging. J. Virol. 74, 8670–8679.

Hobman, T.C., 1993. Targeting of viral glycoproteins to the Golgi complex. Trends Microbiol. 1, 124–130.

Izquierdo-Useros, N., Naranjo-Gomez, M., Erkizia, I., Puertas, M.C., Borras, F.E., Blanco, J., Martinez-Picado, J., 2010. HIV and mature dendritic cells: Trojan exosomes riding the Trojan horse? PLoS Pathog. 6, e1000740.

Jane, D.T., DaSilva, L., Koblinski, J., Horwitz, M., Sloane, B.F., Dufresne, M.J., 2002. Evidence for the involvement of cathepsin B in skeletal myoblast differentiation. J. Cell. Biochem. 84, 520–531.

Jane, D.T., Morvay, L., Dasilva, L., Cavallo-Medved, D., Sloane, B.F., Dufresne, M.J., 2006. Cathepsin B localizes to plasma membrane caveolae of differentiating myoblasts and is secreted in an active form at physiological pH. Biol. Chem. 387, 223–234.

Jin, C., Flavell, R.A., 2010. Molecular mechanism of NLRP3 inflammasome activation. J. Clin. Immunol. 30, 628–631.

Joshi, A., Ablan, S.D., Soheilian, F., Nagashima, K., Freed, E.O., 2009. Evidence that productive human immunodeficiency virus type 1 assembly can occur in an intracellular compartment. J. Virol. 83, 5375–5387.

Jouve, M., Sol-Foulon, N., Watson, S., Schwartz, O., Benaroch, P., 2007. HIV-1 buds and accumulates in "nonacidic" endosomes of macrophages. Cell Host Microbe 2, 85–95.

Jouvenet, N., Neil, S.J., Bess, C., Johnson, M.C., Virgen, C.A., Simon, S.M., Bieniasz, P.D., 2006. Plasma membrane is the site of productive HIV-1 particle assembly. PLoS Biol. 4, e435.

Jouvenet, N., Zhadina, M., Bieniasz, P.D., Simon, S.M., 2011. Dynamics of ESCRT protein recruitment during retroviral assembly. Nat. Cell. Biol. 13, 394–401.

Katunuma, N., 2011. Structure-based development of specific inhibitors for individual cathepsins and their medical applications. Proc. Jpn. Acad. Ser. B Phys. Biol; Sci. 87, 29–39.

Ko, D.C., Gordon, M.D., Jin, J.Y., Scott, M.P., 2001. Dynamic movements of organelles containing Niemann-Pick C1 protein: NPC1 involvement in late endocytic events. Mol. Biol. Cell 12, 601–614.

Kramer, B., Pelchen-Matthews, A., Deneka, M., Garcia, E., Piguet, V., Marsh, M., 2005. HIV interaction with endosomes in macrophages and dendritic cells. Blood Cells Mol. Dis. 35, 136–142.

Kyei, G.B., Dinkins, C., Davis, A.S., Roberts, E., Singh, S.B., Dong, C., Wu, L., Kominami, E., Ueno, T., Yamamoto, A., Federico, M., Panganiban, A., Vergne, I., Deretic, V., 2009. Autophagy pathway intersects with HIV-1 biosynthesis and regulates viral yields in macrophages. J. Cell. Biol. 186, 255–268.

Liscum, L., 2000. Niemann-Pick type C mutations cause lipid traffic jam. Traffic 1, 218–225.

Luzio, J.P., Pryor, P.R., Bright, N.A., 2007. Lysosomes: fusion and function. Nat. Rev. Mol. Cell. Biol. 8, 622–632.

Maekawa, Y., Himeno, K., Katunuma, N., 1997. Cathepsin B-inhibitor promotes the development of Th1 type protective T cells in mice infected with Leishmania major. J. Med. Invest. 44, 33–39.

Matarrese, P., Ascione, B., Ciarlo, L., Vona, R., Leonetti, C., Scarsella, M., Mileo, A.M., Catricala, C., Paggi, M.G., Malorni, W., 2010. Cathepsin B inhibition interferes

with metastatic potential of human melanoma: an in vitro and in vivo study. Mol. Cancer 9, 207.
McGrath, M.E., 1999. The lysosomal cysteine proteases. Annu. Rev. Biophys. Biomol. Struct. 28, 181–204.
Morita, E., Sundquist, W.I., 2004. Retrovirus budding. Ann. Rev. Cell. Dev. Biol. 20, 395–425.
Mullock, B.M., Bright, N.A., Fearon, C.W., Gray, S.R., Luzio, J.P., 1998. Fusion of lysosomes with late endosomes produces a hybrid organelle of intermediate density and is NSF dependent. J. Cell. Biol. 140, 591–601.
Nakatogawa, H., Ichimura, Y., Ohsumi, Y., 2007. Atg8, a ubiquitin-like protein required for autophagosome formation, mediates membrane tethering and hemifusion. Cell 130, 165–178.
Noda, T., Fujita, N., Yoshimori, T., 2009. The late stages of autophagy: how does the end begin? Cell Death Differ. 16, 984–990.
Nydegger, S., Foti, M., Derdowski, A., Spearman, P., Thali, M., 2003. HIV-1 egress is gated through late endosomal membranes. Traffic 4, 902–910.
Ono, A., Freed, E.O., 2004. Cell-type-dependent targeting of human immunodeficiency virus type 1 assembly to the plasma membrane and the multivesicular body. J. Virol. 78, 1552–1563.
Orenstein, J.M., 2002. Ultrastructure of HIV/AIDS. Ultrastruct. Pathol. 26, 245–250.
Palmer, E., Sporborg, C., Harrison, A., Martin, M.L., Feorino, P., 1985. Morphology and immunoelectron microscopy of AIDS virus. Arch. Virol. 85, 189–196.
Pelchen-Matthews, A., Kramer, B., Marsh, M., 2003. Infectious HIV-1 assembles in late endosomes in primary macrophages. J. Cell Biol. 162, 443–455.
Perlman, M., Resh, M.D., 2006. Identification of an intracellular trafficking and assembly pathway for HIV-1 gag. Traffic 7, 731–745.
Qiu, Z., Hingley, S.T., Simmons, G., Yu, C., Das Sarma, J., Bates, P., Weiss, S.R., 2006. Endosomal proteolysis by cathepsins is necessary for murine coronavirus mouse hepatitis virus type 2 spike-mediated entry. J. Virol. 80, 5768–5776.
Raposo, G., Moore, M., Innes, D., Leijendekker, R., Leigh-Brown, A., Benaroch, P., Geuze, H., 2002. Human macrophages accumulate HIV-1 particles in MHC II compartments. Traffic 3, 718–729.
Reefman, E., Kay, J.G., Wood, S.M., Offenhauser, C., Brown, D.L., Roy, S., Stanley, A.C., Low, P.C., Manderson, A.P., Stow, J.L., 2010. Cytokine secretion is distinct from secretion of cytotoxic granules in NK cells. J. Immunol. 184, 4852–4862.
Resh, M.D., 2005. Intracellular trafficking of HIV-1 Gag: how Gag interacts with cell membranes and makes viral particles. AIDS Rev. 7, 84–91.
Sanchez, A., 2007. Analysis of filovirus entry into vero e6 cells, using inhibitors of endocytosis, endosomal acidification, structural integrity, and cathepsin (B and L) activity. J. Infect. Dis. 196 (Suppl 2), S251–258.
Schwartz, S., Campbell, M., Nasioulas, G., Harrison, J., Felber, B.K., Pavlakis, G.N., 1992. Mutational inactivation of an inhibitory sequence in human immunodeficiency virus type 1 results in Rev-independent gag expression. J. Virol. 66, 7176–7182.
Sherer, N.M., Lehmann, M.J., Jimenez-Soto, L.F., Ingmundson, A., Horner, S.M., Cicchetti, G., Allen, P.G., Pypaert, M., Cunningham, J.M., Mothes, W., 2003. Visualization of retroviral replication in living cells reveals budding into multivesicular bodies. Traffic 4, 785–801.
Stow, J.L., Low, P.C., Offenhauser, C., Sangermani, D., 2009. Cytokine secretion in macrophages and other cells: pathways and mediators. Immunobiology 214, 601–612.
Tang, Y., Leao, I.C., Coleman, E.M., Broughton, R.S., Hildreth, J.E., 2009. Deficiency of niemann-pick type C-1 protein impairs release of human immunodeficiency virus type 1 and results in Gag accumulation in late endosomal/lysosomal compartments. J. Virol. 83, 7982–7995.
Toohey, K., Wehrly, K., Nishio, J., Perryman, S., Chesebro, B., 1995. Human immunodeficiency virus envelope V1 and V2 regions influence replication efficiency in macrophages by affecting virus spread. Virology 213, 70–79.
van Ijzendoorn, S.C., 2006. Recycling endosomes. J. Cell Sci. 119, 1679–1681.
Waheed, A.A., Freed, E.O., 2009. Lipids and membrane microdomains in HIV-1 replication. Virus Res. 143, 162–176.
Wehrly, K., Chesebro, B., 1997. P24 antigen capture assay for quantification of human immunodeficiency virus using readily available inexpensive reagents. Methods 12, 288–293.
Weischenfeldt, J., Porse, B., 2008. Bone Marrow-Derived Macrophages (BMM): Isolation and Applications. CSH Protoc 2008, pdb prot5080.
Welsch, S., Groot, F., Krausslich, H.G., Keppler, O.T., Sattentau, Q.J., 2011. Architecture and regulation of the HIV-1 assembly and holding compartment in macrophages. J. Virol. 85, 7922–7927.
Welsch, S., Keppler, O.T., Habermann, A., Allespach, I., Krijnse-Locker, J., Krausslich, H.G., 2007. HIV-1 buds predominantly at the plasma membrane of primary human macrophages. PLoS Pathog. 3, e36.
Williams, R.L., Urbe, S., 2007. The emerging shape of the ESCRT machinery. Nat. Rev. Mol. Cell. Biol. 8, 355–368.
Yoshii, H., Kamiyama, H., Goto, K., Oishi, K., Katunuma, N., Tanaka, Y., Hayashi, H., Matsuyama, T., Sato, H., Yamamoto, N., Kubo, Y., 2011. CD4-independent human immunodeficiency virus infection involves participation of endocytosis and cathepsin B. PLoS One 6, e19352.